This is the author's final accepted version.

There may be differences between this version and the published version. You are advised to consult the publisher's version if you wish to cite from it.

http://eprints.gla.ac.uk/160975/

Deposited on: 16 May 2018

**Sputter-deposited magneto-optical garnet for all mode (transverse electric / transverse magnetic) Faraday rotators**

Bethanie J.H. Stadler and David C. Hutchings

Bethanie J.H. Stadler, University of Minnesota, USA; stadler@umn.edu

David C. Hutchings, University of Glasgow, Scotland; david.hutchings@glasgow.ac.uk

Faraday rotators in optical isolators, typically composed of iron garnets, are photonic analogues of electrical diodes in that they do not allow reciprocal transmission of light. Such isolators are especially important for blocking back-reflected light from reaching source lasers, as such feedback gives rise to unwanted noise and instabilities. In commonly implemented photonic integrated circuits (PICs), isolation is the only critical function that cannot be achieved by direct integration. While techniques have been explored for integrating high-gyrotropy garnets into silicon-on-insulator (SOI) PICs, this article will focus on sputter deposition, which is the most up-scalable process. High-gyrotropy Ce-doped yttrium iron garnet (YIG) on nongarnet substrates can be made by sputter deposition with the use of garnet seed layers. Because these seed layers can compromise device performance, seed layer-free terbium iron garnet (TIG) has also recently been developed. Careful doping of TIG can produce Faraday rotations with opposite chiralities, which enable new device designs. Most optical isolator designs involve two-dimensional transverse magnetic-mode structures, such as interferometers or ring resonators, which employ nonreciprocal phase shift. One-dimensional Faraday rotation waveguides with quasi-phase matching have been shown to enable direct integration of isolators for all modes, including the transverse electric -mode lasers currently available for fully integrated PICs.

**Elements of a Faraday rotator**

Nonreciprocal optical isolators are necessary and ubiquitous components in optical fiber systems, primarily using Faraday rotation of linearly polarized light to protectg laser sources from back reflections, which can cause unwanted noise and instabilities (**Figure 1**a). Typical implementations of optical isolators involve the assembly of discrete elements (eg: pieces of garnet) into a single optical-fiber-coupled device without waveguiding structures (Figure 1b). Integrated photonics is a new field that offers a route to mass production of multiple isolator devices on a single chip, and also to realize photonic integrated circuits (PICs) where lithography and microfabrication are used to define and align elements, similar to electronic integrated circuit (ICs). Unfortunately, isolators and other devices that break time-reversal symmetry are not currently available in PIC systems,[2] such as silicon-on-insulator (SOI) chips.

Unlike fiber isolators, PIC devices consist of waveguide structures, and the light (also called, electromagnetic waves) is guided in modes whose polarization is defined by the alignment between the electric field of the light and the plane of the chip. Implementing nonreciprocity therefore involves additional complexities[3] (**Figure 2**a). Most integrated lasers emit transverse electric (TE)-polarized modes (electric field lies predominantly in the plane of the chip), and a majority of integrated PIC devices also operate in the TE mode. An ideal integrated isolator should allow forward propagation of TE-polarized modes, and it should either convert reflections to transverse magnetic (TM) polarization (electric field lies predominantly normal to the plane of the chip), which does not normally interact with TE-mode (quantum well) lasers, or block reflections altogether.

Many proposed integrated isolators use nonreciprocal phase shift (NRPS), a phenomenon that induces a phase shift in TM-polarized modes using a transverse magnetic field, rather than the longitudinal magnetic field shown in Figure 1. NRPS structures are two-dimensional (2D) because they are either branched interferometers[4,5] or ring resonators.[6,7]   Garnet claddings are introduced

to these structures via vacuum deposition, such as pulsed layer deposition (PLD), or wafer bonding, both of which locate the garnet more easily on top of the waveguides. Some attempts have been made to tilt samples during PLD for sidewall coating which enables TE functionality[8,9.] More often, these devices require reciprocal polarization converters (RPC) before and after the isolator[5] to convert TE modes into TM modes (for NRPS isolation) and then back to TE modes (for transmission into the circuit). Full reciprocal modal conversion is more difficult[5] to implement than half reciprocal conversion,[10] but with just one half RPC and a garnet top-cladded waveguide, a Faraday rotation isolator is complete, as described below.[10,11]

The waveguide equivalence of Faraday rotation is nonreciprocal mode conversion because the changing polarization is manifested as the light energy flowing from a TE-mode into a TM-mode. Waveguides are typically birefringent because the propagation constants of the TE- and TM-polarized modes do not match, for example, due to shape anisotropy where the waveguide height is much less than its width. These dimensions are easier to fabricate and are favorable to break mode degeneracy, but the modal phase mismatch inhibits nonreciprocal phase conversion resulting in a periodic behavior of limited magnitude and beat length corresponding to an accumulated modal phase difference of $\Delta\phi = 2\pi$ (sine-like curve in Figure 2b).

A simple solution to phase mismatch is quasi-phase matching (QPM),[10,12] which compensates for the phase velocity mismatch and ensures a monotonic flow of energy between the coupled modes (step-like curve in Figure 2b). QPM requires that the waveguide (Figure 2b, inset) be periodically modulated to suspend Faraday rotation during the downswing of each beat length, as shown. This alternating of magneto-optic garnet with nonchiral materials involves lengths $L_G$ and $L_N$, respectively, such that the accumulated modal phase difference $\Delta\phi = 2\pi$ (for first-order QPM) over the propagation distance ($L_G+L_N$) to compensate birefringence as shown.

To visualize the polarization state of the light, Stokes parameters ($S_1$, $S_2$, and $S_3$) can be plotted on the surface of the Poincaré sphere which is shown in

Figure 2c.[10] Linear polarization states correspond to the "equator," circular polarization states correspond to the "poles," and Faraday rotation is equivalent to moving around the equator. For an isolator, the backward output (e.g., TM polarized) should ideally be orthogonal to the forward injected light (e.g., TE polarized), so the angle between the input and output Stokes vectors is $\pi$ radians. A full SOI-compatible isolator[3] involves a QPM cladding on a Si waveguide (Figure 2d). Experimental verification of this design is discussed at the end of this article where this sphere will be used to explain the state of the light as it travels through the device. Note: this article deals with SOI photonics so optical properties are all reported for near infrared (1.55 μm).

**Sputter deposition of garnet on nongarnet substrate**

The garnets used in optical fiber isolators (Figure 1c) are thick films of yttrium iron garnet (YIG) doped with Bi, Ce, and other elements to improve gyrotropy (a term that includes all nonreciprocal effects, such as Faraday rotation and NRPS), temperature stability, and, in some cases, to provide perpendicular magnetic anisotropy in order to negate the need for a permanent magnet. These films are grown by liquid-phase epitaxy from a molten lead oxide solute. This process is incompatible with integrated photonics on Si. Initial attempts to grow YIG films on Si-compatible substrates by vacuum processes often resulted in small cracks in the YIG films.[13] For early applications, such as proposed bubble memory for computers, these micro-cracks were somewhat acceptable.[14] However, light cannot propagate through a garnet waveguide if it contains any cracks, and cracked garnet claddings on Si waveguides would cause unacceptable optical losses.

In 2005, a process was discovered by which YIG could be grown on nongarnet substrates, including Si, by sputter deposition, lithography, and then rapid thermal annealing (RTA).[15] This process mitigated thermal expansion mismatches between SOI-compatible materials ($\alpha_{SiO_2} = 0.5$ ppm/°C, $\alpha_{Si} = 2.33$ ppm/°C) and garnet ($\alpha = 10.4$ ppm/°C), and waveguide losses were measured to be less than 1 dB/mm.[16] Attempts to dope this YIG, however, were unsuccessful

due to the formation of secondary phases, until thin layers of undoped YIG (prepared similar to the 2005 method) were used as seed layers for pulsed laser deposited (PLD) Ce-doped YIG (Ce:YIG).[6] It is important to dope YIG because the Faraday rotation, which stems from the off-diagonal components of the dielectric matrix, is greatly increased (although opposite in sign). For example, the Faraday rotation of undoped YIG in bulk and films has been reported[17] to be +200 degrees/cm, but the (absolute) value is increased to –4500 degrees/cm in sputtered Ce:YIG on gadolinium gallium garnet (GGG) substrates.[18] For most isolator configurations, the absolute value of the Faraday rotation is more important than the sign, or chirality. For iron garnets, the diagonal terms in the dielectric matrix are the square of the refractive index and have a typical value $n^2$ = 4.41.

Follow-up studies of seed layer and annealing methods have been conducted by many groups, some of which are covered by Ross in this issue. Here, we call attention to two important discoveries—optimal seed layer thickness[19] via RTA and a two-step anneal to enable thinner seed layers.[20] Both of these studies showed the importance of direct observation of crystallinity, for example, by electron backscattered diffraction (EBSD), (**Figure 3**a[19]) or transmission electron microscopy (TEM), (Figure 3b–c[20]). X-ray diffraction (XRD) alone does not show the presence of nanocrystalline or amorphous phases.

Since 2005, RTA has been used as a fast, Si-compatible method to crystallize garnet films. In crystallization studies,[19] at thicknesses below a minimum value of 45 nm, YIG failed to crystallize fully, which resulted in incomplete crystallization of the Ce:YIG claddings, as seen in Figure 3a. Seed layers above 45 nm yielded the largest Faraday rotation to date for monolithically integrated Ce:YIG on Si (–3700 degrees/cm).[19] Although epitaxial films on GGG have slightly larger gyrotropies, monolithic integration with Si photonics will make upscaling PICs more facile than hybrid integration of garnet-on-garnet.

A second crystallization study showed that very thin (25 nm) YIG films can be fully crystallized without increasing the energy (thermal processing) budget by using a two-step approach.[20] *In situ* crystallization was studied by TEM

using laser pulses to anneal 25-nm-thick YIG films. Low temperature (400°C) "pre-anneals" followed by typical 800°C annealing, enabled YIG crystallites to experience growth fronts of 280 nm/s. In this way, the entire film was crystallized into garnet before the typical nanocrystalline matrix could be formed. These *in situ* TEM crystallization results were then verified by rapid thermal annealing (Figure 3b–c).

For garnet-core waveguide devices, sputter-deposited films of Ce:YIG on various seed layers are excellent options for nonreciprocal devices using thick bottom claddings on Si. In fact, full isolation can be achieved with path lengths as short as 350 μm (**Figure 4**), even when large waveguide birefringence is large.[17,21] As in electronic ICs, small devices are desireable for PICs to achieve more functionality per chip. The structures in Figure 4 are the same as shown in Figure 2b, but here, the "nongarnet" segments are replaced with opposite chirality garnets to create "push/pull" Faraday rotators. In this case, the Faraday rotation is not suspended, but rather the periodic downswings in the beat-length become upswings to enable devices with very short path lengths. For example, undoped TIG has a Faraday rotation (+500 degrees/cm) that is 2.5× larger than for YIG (+200 degrees/cm). Bi doping of TIG (Bi:TIG) produces a similar magnitude, but opposite chirality Faraday rotation (–500 degrees/cm). As future garnets are discovered with enhanced Faraday rotation of both chiralities, even shorter Faraday rotators will be possible regardless of waveguides birefringence.

A large number of integrated photonic devices have been realized with SOI platforms where light propagates inside Si-core waveguide devices. Si has diagonal dielectric components of $n^2 = 11.7$, so there will be large reflections at any interface that requires the light to propagate from a Si core to a garnet core. Therefore, garnet-clad SOI waveguides are necessary to provide isolators for Si PICs, whether those isolators use NRPS or Faraday rotation. However, the best Ce:YIG films on Si are made using a seed layer that is located between the Si and the Ce:YIG (**Figure 5**). When using Ce:YIG as a cladding, isolation is dependent on the interaction between the evanescent field of the light which 'leaks' outside the Si core into this cladding. As seen in Fig. 5, the evanescent interaction

decreases exponentially with distance from the Si core (contour lines show -3dB intervals), so a dilemma is introduced: thin seed layers are desired to enable more evanescent interaction with the Faraday rotation of the Ce:YIG cladding, but thicker seed layers are needed to fully crystallize Ce:YIG (and therefore obtain higher Faraday rotation). Sidewall coatings were mentioned above for TE-mode NRPS operation, but this simulation shows the waveguides will also need to careful design to enable side 'leakage' for this to work. For direct contact between Ce:YIG cladding and Si core, new top seed layers[22] and creative geometries have also been used to avoid mid-structure seed layers, but device fabrication will be greatly simplified using seed layer-free garnet.

Undoped and doped terbium iron garnets (TIG)[17,21] meet this need of not requiring a seed layer to form on Si. Also, the chirality of the rotation of Bi:TIG matches Ce:YIG, and therefore, it can be a  Ce:YIG seed layer that is better than undoped YIG.[17] Interestingly, despite the low values of Faraday rotation, Bi:TIG has been shown to enable higher performance in SOI devices than Ce:YIG (see next section). Seed layers introduce extra annealing and extra lithography steps, so single deposition TIG-based films are gaining popularity. Ce:TIG has recently been reported with Faraday rotations of –2600 degrees/cm,[21] and this material is now being explored as a cladding on many proprietary SOI designs.

**Faraday rotation in SOI waveguide devices: All-mode isolation**

TE-mode SOI-integrated isolators were recently realized with a uniform longitudinal magnetization causing Faraday rotation (FR).[3] These SOI FR isolators were similar in length to TM-mode NRPS Mach–Zehnder interferometers (MZI) and ring resonators, but the FR isolators are essentially 1D (all in a continuous line), which allows very high device densities. FR isolators only require two elements for TE-mode operation: a FR and a half reciprocal polarization converter (RPC) (Figure 2d). Recall that the isolator must transmit TE-mode light from the laser into the PIC chip. But it must also convert all (unwanted, unintentional) back reflections from the chip into TM-mode light so that these reflections will not interfere with the performance of the laser. Here is how it works. The FR is designed to allow half of the light energy to flow into the

TM-mode in the forward direction (purple to blue equator motion in Figure 2c). The half RPC is used to convert the (TE = TM) output of the FR back to full TE mode before the light continues into the photonic integrated circuit (lower dashed curve in Figure 2c). This half converter is more straightforward to realize than a full converter.[13] Any backward traveling light propagates first through the half RPC and then through the FR (top dashed curve, then yellow to green equator motion in Figure 2c). So, these reflections first split their energy (TM=TE) and then FR to full TM-modes before they reach the laser, leading to a Stokes vector angle of $\pi$ radians (difference between $S_1 = 1$ and -1). An additional waveguide polarization-selective element could be included between the laser and the FR, as in Figure 1, but here, the polarization selectivity of the quantum well laser itself makes it essentially transparent to TM-polarized light at the wavelength of operation.

Quasi-phase matching (Figure 2b) was accomplished by periodic liftoff lithography of the garnet cladding,[23] and then by coating the waveguide with $Si_xN_y$ for approximate index matching to produce segment lengths corresponding to the characteristic beat length ($L_G + L_N$). Silicon-on-insulator (340-nm-thick Si) deep-reactive-ion-etched waveguides were patterned using electron-beam-written poly(methyl methacrylate) masks with liftoff after garnet deposition. Several garnet claddings were used, including Ce:YIG on YIG (45nm) and seed layer-free Bi:TIG (80-nm thick). The best results were obtained with Bi:TIG[3] even though simulations had indicated that the Ce:YIG claddings should perform better.[17] Presumably this was due to the simplicity of fabrication, which minimizes errors from multiple lithography and annealing steps.

Isolation by nonreciprocal photonic devices is reported as the ratio between TM-polarized transmission in the forward and backward directions, which is usually inferred from the equivalent measurement of the difference in TM-polarized forward transmission when the transverse magnetic fields are reversed. This "equivalent" measurement eliminates error caused by experimental variations when coupling  light into the input vs output of the device. A Stokes vector angle of 0.83 $\pi$ was found for the best of the first-generation Faraday

rotation isolators that were 3.4-mm long.[3] Optimization is underway, but even for these non-optimized devices, simply extending the device lengths to 4.1 mm would be appropriate to obtain a Stokes vector angle close to the ideal value of $\pi$. The QPM period ($L_G + L_N$) corresponding to the results shown in **Figure 6** was 8 µm (SOI core: 340 nm × 900 nm), which is a resolution that is easily achieved with standard photolithography. Importantly, with a Stokes vector angle of 0.83 $\pi$, a maximum isolation ratio of –11 dB[3] could be obtained, which is similar to ratios obtained with first reports of TM-mode isolator designs.

## Summary

Similar to the ubiquitous isolators in current fiber optic systems, Faraday rotators enable source-integrated photonic circuit systems by mitigating reflections to reduce laser feedback and noise. The waveguide equivalent of Faraday rotation, nonreciprocal mode conversion, can be used in 1D (in-line) SOI waveguides simply by providing a top cladding of garnet and a longitudinal magnetic field. Quasi-phase matching can be used to overcome waveguide birefringence while maintaining shape anisotropy, for example, a typical SOI waveguide core (cross section: 340 nm × 900 nm) was clad with alternating segments of Ce:YIG/YIG or Bi:TIG separated by segments of SiN$_x$. Successful all-mode (TE to TM) isolators were measured with -11.6 dB isolation ratios and losses of only 4.6 dB. By extending the length of the Bi:TIG/SiN$_x$-cladded SOI guides from 3.6 mm to 4.1 mm, simulations show nearly perfect isolation and only 5 dB loss. With these results, source-integrated PICs should be available in the near future.

## Acknowledgments

## References

1. www.thorlabs.com/Optics/Isolators

2. B.J.H. Stadler, T. Mizumoto, *IEEE Photonics J.* **6**, 0600215 (2014).

3. C. Zhang, P. Dulal, B.J.H. Stadler, D.C. Hutchings, *Nat. Sci. Rep.* **7** (5820), 1 (2017).

4. Y. Shoji, Y. Shirato, T. Mizumoto, *Jpn. J. Appl. Phys.* **53**, 022202 (2014).

5. S. Ghosh, S. Keyvaninia, Y. Shoji, W. Van Roy, T. Mizumoto, G. Roelkens, and R. G. Baets*IEEE Photonics Technol. Lett.* **24**, 1653 (2012).

6. L. Bi, J. Hu, P. Jiang, D.H. Kim, G.F. Dionne, L.C. Kimerling and C.A. Ross, *Nat. Photonics* **5**, 758 (2011).

7. M.-C. Tien, T. Mizumoto, P. Pintus, H. Kromer, J.E. Bowers, *Opt. Express* **19**, 11740 (2011).

8. P. Pintus, F. Di Pasquale, J.E. Bowers, *Opt. Lett.* **36**, 4599 (2011).

9. H. Shimizu, Y. Nakano, *J. Lightwave Technol.* **24**, 38 (2006).

10. D.C. Hutchings, B.M. Holmes, *IEEE Photonics J.* **3**, 450 (2011).

11. D.C. Hutchings, *J. Phys. D Appl. Phys.* **36**, 2222 (2003).

12. P.K. Tien, R.J. Martin, R. Wolfe, R.C.L. Craw, S.L. Blank, *Appl. Phys. Lett.* **21**, 394 (1972).

13. L.J. Cruz-Rivera, S.-Y. Sung, J. Cassada, M.R. Marrero-Cruz, B.J.H. Stadler, *Mater. Res. Soc. Symp. Proc.* **722**, R.B. Wehrspohn, R. März, S. Noda, C. Soukoulis, Eds. (Materials Research Society, Warrendale, PA, 2002), p. 262.

14. M. Abe, M. Gomi, *J. Magn. Magn. Mater.* **84**, 222 (1990).

15. S.-Y. Sung, X. Qi, B.J.H. Stadler, *Appl. Phys. Lett.* **87**, 121111 (2005).

16. S.-Y. Sung, A. Sharma, A. Block, K. Keuhn, B.J.H. Stadler, *J. Appl. Phys.* **109**, 07B738 (2011).

17. P. Dulal, A.D. Block, T.E. Gage, H.A. Haldren, S.-Y. Sung, D.C. Hutchings, B.J.H. Stadler, *ACS Photonics* **3**, 1818 (2016).

18. Y. Shoji, T. Mizumoto, H. Yokoi, I.W. Hsieh, R.M. Osgood, *Appl. Phys. Lett.* **92**, 071117 (2008).

19. A.D. Block, P. Dulal, B.J.H. Stadler, N.C. Seaton, *IEEE Photonics J.* **6**, 0600308 (2014).

20. T.E. Gage, P. Dulal, P.A. Solheid, D.J. Flannigan, B.J.H. Stadler, "Si-Integrated Ultrathin Films of Phase-Pure Yttrium Iron Garnet via Novel Two-Step Rapid Thermal Anneal" *Mater. Res. Lett.* 1–7 (2017).

21. P. Dulal, T.E. Gage, A.D. Block, E. Cofell, D.C. Hutchings, B.J.H. Stadler, *2016 IEEE Photonics Conference* (2016), p. 773.

22. X.Y. Sun, Q. Du, T. Goto, M.C. Onbasli, D.H. Kim, N.M. Aimon, J. Hu, C.A. Ross, *ACS Photonics* **2**, 856 (2015).

23. D.C. Hutchings, B.M. Holmes, C. Zhang, P. Dulal, A.D. Block, S.-Y. Sung, N.C.A. Seaton, B.J.H. Stadler, *IEEE Photonics J.* **5**, 6602512 (2013).

**Figure Captions**

**Figure 1.** (a) Operation of a generic Faraday rotation isolator. Linearly polarized laser light propagates forward and experiences 45° Faraday rotation before entering the optical system. From the perspective of the source laser, back reflections rotate in the same direction and are blocked by the polarizer. From the perspective of the propagating light, the rotation has the opposite chirality as it travels forward (with the magnetization of the garnet) versus backward (against the magnetization). (b) Commercial optical-fiber-coupled isolator[1] with schematic showing discrete components inside.

**Figure 2.** (a) Ideal integrated isolators should work for transverse electric (TE)-mode light, meaning they allow TE modes to pass into the photonic integrated circuit (PIC), and then they either convert backward propagating light into transverse magnetic (TM) modes, which do not normally interact with integrated TE-mode lasers, or they block backward propagating light altogether. (b) Schematic showing both the effects of phase velocity mismatch (birefringence, shown in the sine-like curve) and the solution—quasi-phase matching (QPM).[3] QPM can be used to periodically suspend Faraday rotation (steps in second curve), or more specifically, mode conversion, by spatially varying the waveguide (or cladding) such that the period ($L_G + L_N$) corresponds to a modal phase offset of $\Delta\phi = 2\pi$. (Inset) Schematic of a QPM waveguide with extreme shape-induced birefringence (height << width) to demonstrate the scale of a QPM solution: $L_G = L_N = 3.85\mu m$, easily fabricated with simple photolithography.[3] (c) Poincaré sphere representation of polarization states of propagating modes with nonreciprocal (solid lines) and reciprocal phase shifts (dashed lines). $S_1$, $S_2$, and $S_3$ are Stokes parameters. (d) Schematic of silicon-on-insulator integrated isolator using a simple waveguide with QPM garnet claddings for nonreciprocity that is fully TE functional with the addition of a simple half-reciprocal phase converter [3].

**Figure 3.** (a) Electron backscattered diffraction of partially crystallized, very thin yttrium iron garnet (YIG) films.[19] (b) Bright-field transmission electron microscope images of 25-nm YIG films annealed at only 800°C for 3 min and (c) first annealed at 400°C for 3 min and subsequently annealed at 800°C for 3 min.[20] Note: dark wavy lines are Moiré fringes due to a slight curvature in otherwise perfect YIG crystallites.

**Figure 4.** Finite-Difference Time Domain (FDTD) simulations of terbium iron garnet (TIG), QPM TIG, and different combinations of push–pull garnet waveguides of 1.6 μm × 0.8 μm cross section (FR, Faraday rotator). The QPM and push–pull waveguides have 3.85-μm-long strips on a fused quartz substrate.[17]

**Figure 5.** Transverse mode profiles for the quasi-TE and quasi-TM fundamental modes in a 340 nm × 900 nm silicon-on-insulator waveguide with 20-nm yttrium iron garnet seed layer and 80 nm of Ce:YIG as an upper cladding. The irradiance contours are shown at –3 dB intervals.

**Figure 6.** Performance of a 340-nm silicon-on-insulator Faraday rotation isolator with seed layer-free Bi:TIG claddings. (Top) The Stokes vector angle of opposite magnetic saturation, where a peak relative angle of 0.83 π is observed. (Bottom) Calculated isolation ratios using this data with an idealized wave plate for reciprocal polarization conversion.

**Bethanie J.H. Stadler** is a professor and associate head of electrical and computer engineering and a graduate faculty member of chemical engineering and materials science at the University of Minnesota. She earned her BS degree in 1990 from Case Western Reserve University, her PhD degree in 1994 from Massachusetts Institute of Technology, and was a National Research Council postdoctoral researcher. She has received a National Science Foundation CAREER Award and a McKnight Presidential Fellowship. She served on the MRS Board of Directors (as a member and as secretary), and she is currently chair of the MRS Program Development Subcommittee. She taught at the IEEE Magnetic Summer School in Chennai, India, and Assisi, Italy. Her current research focuses on integrating photonic and magnetic materials for photonic isolators, modulators, and sensors. She was a 2015 Distinguished Lecturer for the IEEE Magnetics Society. She is a 2018 *MRS Bulletin* Volume Organizer. Stadler can be reached by email at stadler@umn.edu.

**David C. Hutchings** has been a personal chair in optical and quantum electronics at the University of Glasgow, Scotland, since 2004. He obtained his BSc degree in 1984 and his PhD degree in physics in 1988, both from Heriot-Watt University,

Scotland. Following postdoctoral research at The College of Optics and Photonics, University of Central Florida, he held Fellowships at the University of Glasgow from the Royal Society of Edinburgh and Scottish Office/Executive (1992–1995, 2003) and EPSRC (1995–2000). He is a Fellow of the Institute of Physics and senior member of the Institute of Electrical and Electronics Engineers. His current research focuses on nonlinear optics, monolithic and heterogeneous optoelectronic integration, semiconductor theory and modeling, and computational electromagnetics. Hutchings can be reached by email at david.hutchings@glasgow.ac.uk.
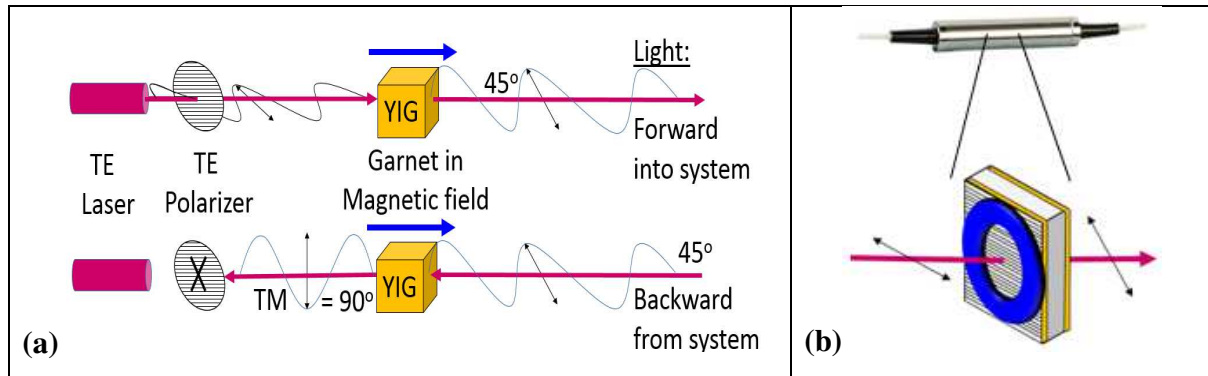
**Figure 1.** (a) Operation of a generic Faraday rotation isolator. Linearly polarized laser light propagates forward through a matching polarizer and is Faraday rotated 45° by the magneto-optic garnet before transmission into the optical system (eg: a fiber optic network). From the perspective of the source laser, back reflections rotate in the same direction as the forward beam, and are blocked by the polarizer. From the perspective of the propagating light, the rotation has the opposite chirality as it travels forward (with the magnetization of the garnet) versus backward (against the magnetization). (b) Commercial optical-fiber-coupled isolator[1] with schematic showing discrete components inside: ring magnet, plastic polarizer film, and magneto-optical garnet films on garnet substrate.
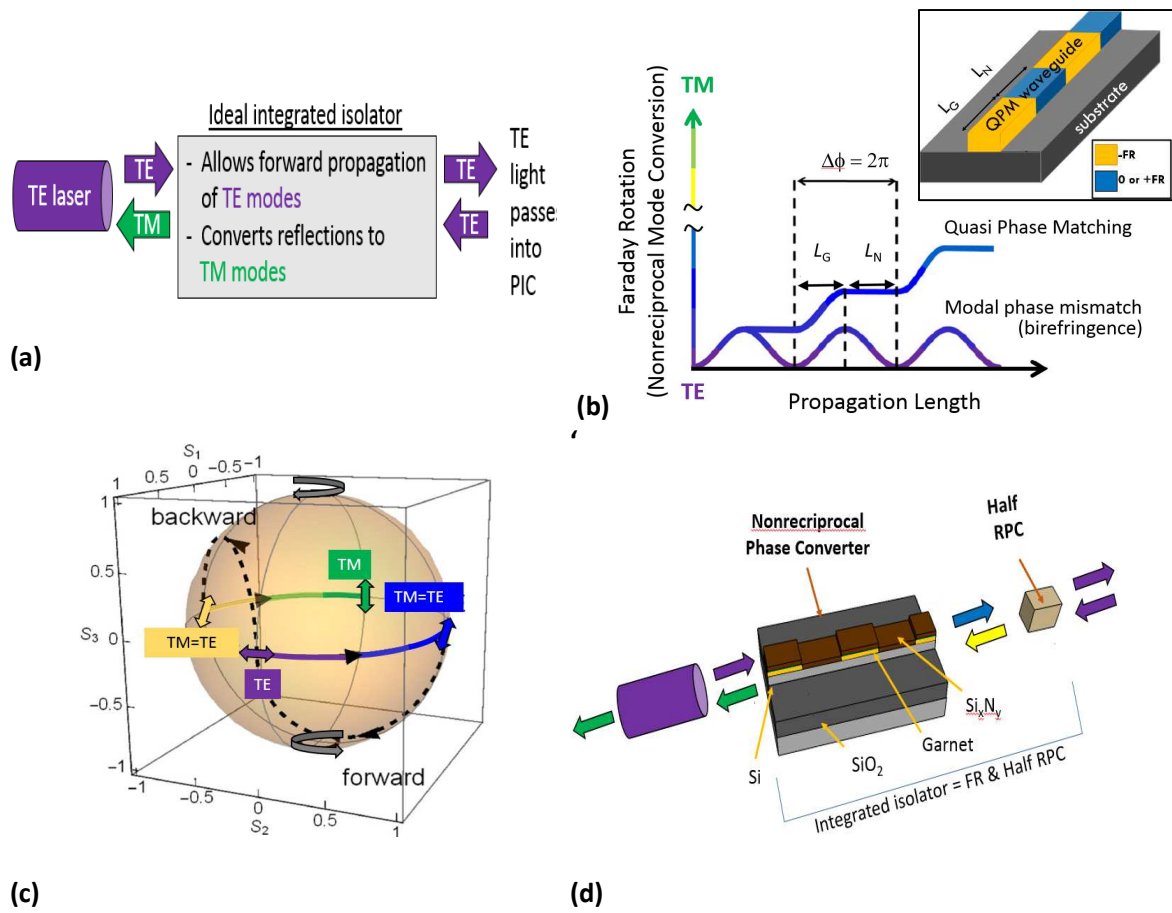
**Figure 2.** (a) Ideal integrated isolators should work for transverse electric (TE)-mode light, meaning they allow TE modes to pass into the photonic system, e.g.: an integrated circuit (PIC), and they either convert backward propagating light into transverse magnetic (TM) modes, which do not interact with integrated TE-mode lasers. (b) Schematic showing both the effects of phase mismatch (birefringence), shown in the sine-like curve, and the solution—quasi-phase matching (QPM).[3] QPM can be used to periodically suspend Faraday rotation (mode conversion), steps-like curve, by spatially varying the waveguide (inset) such that the period ($L_G + L_N$) corresponds to a modal phase offset of $\Delta\varphi = 2\pi$.[3] (c) Poincaré sphere representation of polarization states of propagating modes with nonreciprocal (solid lines) and reciprocal (dashed lines) phase shifts. $S_1$, $S_2$, and $S_3$ are Stokes parameters. (d) Schematic of silicon-on-insulator integrated isolator using a simple waveguide with QPM garnet claddings for nonreciprocity that is fully TE functional with the addition of a simple half-reciprocal phase converter [3].
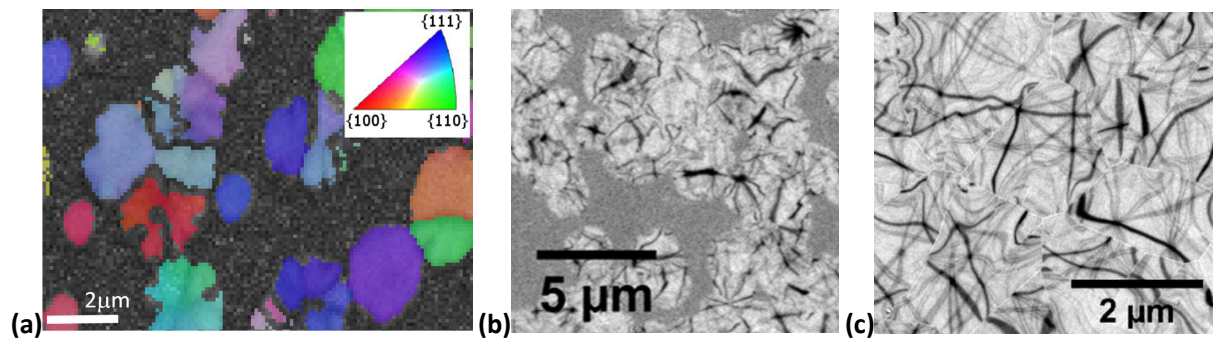
**Figure 3.** (a) Electron backscattered diffraction of partially crystallized, very thin (35nm) yttrium iron garnet (YIG) films.[19] (b) Bright-field transmission electron microscope images of 25-nm YIG films annealed at only 800°C for 3 min and (c) first annealed at 400°C for 3 min and subsequently annealed at 800°C for 3 min, the latter being fully crystallized.[20] Note: dark wavy lines are Moiré fringes due to a slight curvature in otherwise perfect YIG crystallites.
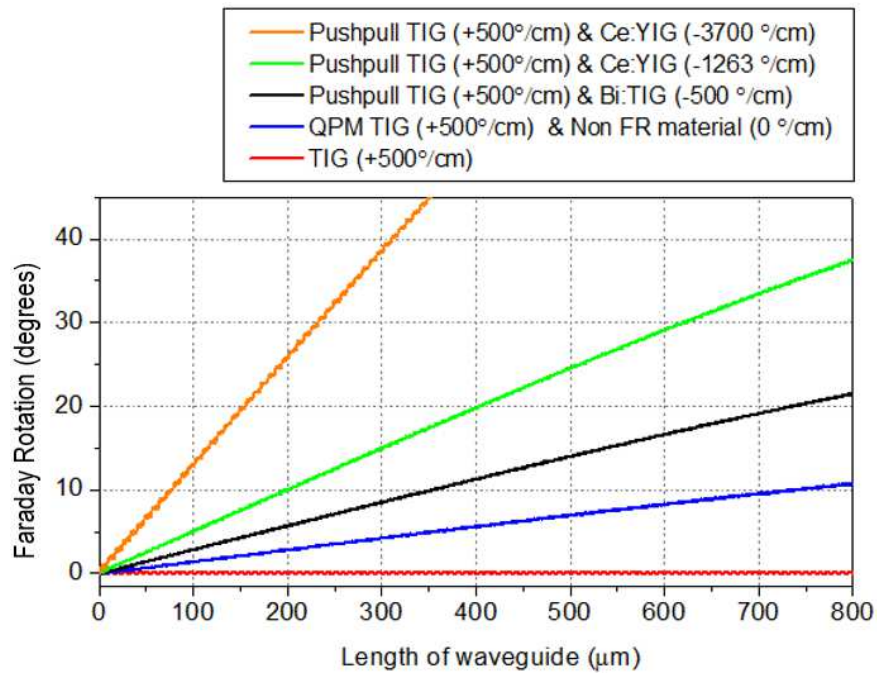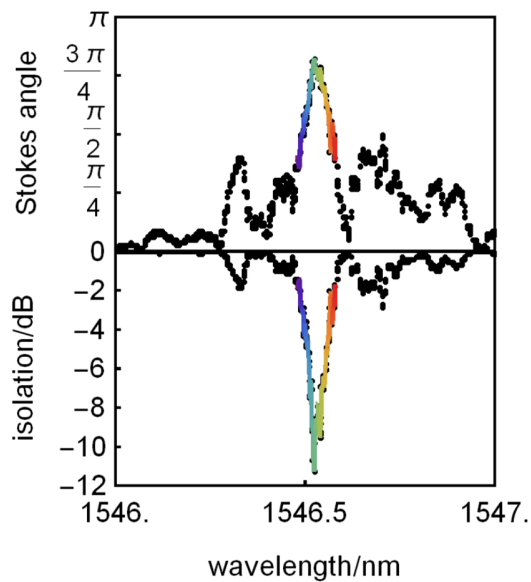
**Figure 4.** Finite-Difference Time Domain (FDTD) simulations of terbium iron garnet (TIG), QPM TIG, and different combinations of push−pull garnet waveguides of 1.6 μm × 0.8 μm cross section (FR, Faraday rotator). The QPM and push−pull waveguides have 3.85-μm-long strips on a fused quartz substrate.[17]
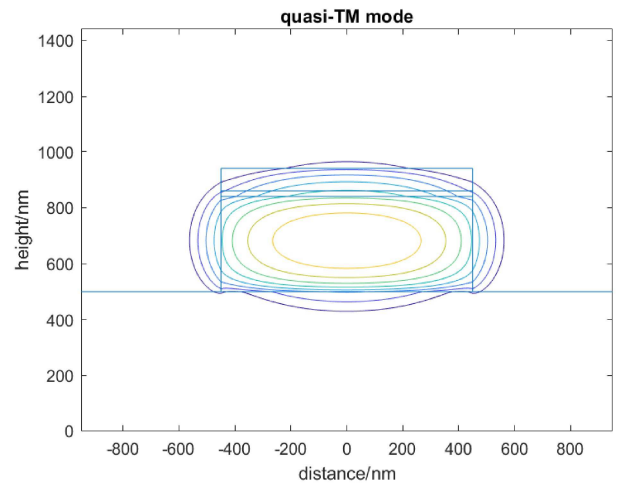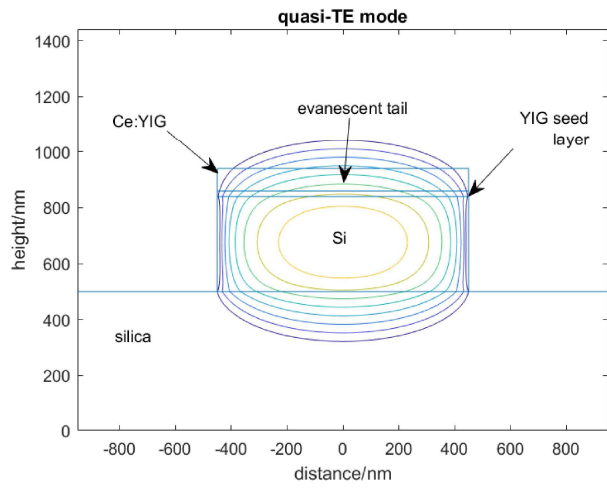
**No change to figure itself, just discussion in text as in comments**

**Figure 5.** Transverse mode profiles for the quasi-TE and quasi-TM fundamental modes in a 340 nm × 900 nm silicon-on-insulator waveguide with 20-nm yttrium iron garnet seed layer and 80 nm of Ce:YIG as an upper cladding. The irradiance contours are shown at –3 dB intervals.



**Figure 6.** Performance of a 340-nm silicon-on-insulator Faraday rotation isolator with seed layer-free Bi:TIG claddings. (Top) The Stokes vector angle of opposite magnetic saturation, where a peak relative angle of 0.83 π is observed. (Bottom) Calculated isolation ratios using this data with an idealized wave plate for reciprocal polarization conversion.